



Article

Effect of Mechanically Exfoliated Graphite Flakes on Morphological, Mechanical, and Thermal Properties of Epoxy

Ayşenur Gül ^{1,2} and Ali Reza Kamali ^{2,3,*}

- ¹ Department of Mechanical Engineering, Işık University, İstanbul 34980, Türkiye; aysenur.gul@isikun.edu.tr
² Department of Materials Science and Metallurgy, University of Cambridge, 27 Charles Babbage Road, Cambridge CB3 0FS, UK
³ Energy and Environmental Materials Research Centre (E²MC), School of Metallurgy, Northeastern University, Shenyang 110819, China
* Correspondence: ali@mail.neu.edu.cn or a.r.kamali@cantab.net

Abstract: Carbon-reinforced polymer composites form an important category of advanced materials, and there is an increasing demand to enhance their performance using more convenient and scalable processes at low costs. In the present study, graphitic flakes were prepared by the mechanical exfoliation of synthetic graphite electrodes and utilized as an abundant and potentially low-cost filler to fabricate epoxy-based composites with different additive ratios of 1–10 wt.%. The morphological, structural, thermal, and mechanical properties of these composites were investigated. It was found that the thermal conductivity of the composites increases by adding graphite, and this increase mainly depends on the ratio of the graphite additive. The addition of graphite was found to have a diverse effect on the mechanical properties of the composites: the tensile strength of the composites decreases with the addition of graphite, whilst their compressive strength and elastic modulus are enhanced. The results demonstrate that incorporating 5 wt% of commercially available graphite into epoxy not only raises the thermal conductivity of the material from 0.223 to 0.485 W/m·K, but also enhances its compressive strength from 66 MPa to 72 MPa. The diverse influence of graphite provides opportunities to prepare epoxy composites with desirable properties for different applications.

Keywords: epoxy resin; thermal conductivity; elastic modulus; graphite; compressive strength; tensile strength



Citation: Gül, A.; Kamali, A.R. Effect of Mechanically Exfoliated Graphite Flakes on Morphological, Mechanical, and Thermal Properties of Epoxy. *J. Compos. Sci.* **2024**, *8*, 466. <https://doi.org/10.3390/jcs8110466>

Academic Editor: Hamed Aghajani Derazkola

Received: 26 September 2024
Revised: 30 October 2024
Accepted: 8 November 2024
Published: 11 November 2024



Copyright: © 2024 by the authors. Licensee MDPI, Basel, Switzerland. This article is an open access article distributed under the terms and conditions of the Creative Commons Attribution (CC BY) license (<https://creativecommons.org/licenses/by/4.0/>).

1. Introduction

Epoxy resins, classified as thermosetting polymers, are widely used as the matrix for advanced polymer-based materials owing to their appropriate mechanical properties, low shrinkage, and excellent adhesion to substrates, as well as their chemical resistance, low cost, lightweight, and manufacturability [1]. Moreover, they are thermal and electrical insulators and transparent to electromagnetic radiations, making them attractive for a number of applications such as heavy-duty anticorrosion coating [2], structural adhesive [3], and biomedical systems [4].

However, the insulating nature of resins is a barrier against their usage in thermal management applications [5] in which conductivity is important. In order to mitigate this limitation, there are growing research activities aiming to improve the thermal/electrical properties of resins for a range of applications [6]. In this regard, adding appropriate fillers to the resin is an effective and convenient way to obtain composite materials with multifunctional properties such as increased thermal and electrical conductivity as well as improved mechanical and barrier properties. A great deal of investigations has been conducted on modifying the properties of epoxy by adding different types of fillers, such as alumina (Al₂O₃) [7], silicon carbide (SiC) [8], and boron carbide (B₄C) [9], enabling us to improve the mechanical properties of epoxy. Moreover, additives such as molybdenum

sulfide (MoS₂) [10] and polytetrafluoroethylene [11] make epoxy suitable for use in low-friction and low-wear environments.

It has been found that carbon fillers such as carbon nanotubes [12], graphene/graphene oxide [13], and expanded graphite [14] may increase the mechanical, thermal, and electrical properties of native polymers. Although underestimated in the literature, graphite, a three-dimensional pure form of carbon with a layered hexagonal crystalline form, can be an attractive filler in comparison with carbon nanotubes and graphene because of its low cost and high availability. In graphite, the covalent carbon sp² bonds along the pristine graphitic sheets can provide thermal and electrical conductivity as well as excellent chemical stability and lubricant properties. Despite the interesting features of graphite, its application in epoxy-based composites has been underestimated in comparison with considerably more expensive and environmentally problematic alternatives. In particular, the mechanical exfoliation of graphite [15] can lead to the preparation of graphitic flakes that can potentially act as ideal fillers for enhancing the thermal and mechanical properties of polymer composites. Other possible approaches, which typically involve increased costs, include molten salt exfoliation [16], liquid-phase exfoliation [17], and chemical vapor deposition [18].

Epoxy resins generally have low thermal conductivity; however, incorporating graphite derivatives such as expanded graphite [19,20], graphene nanoplatelets [21], and graphene oxide [22] can enhance this property. Furthermore, the mechanical properties of epoxy-based materials can be altered by the addition of carbon materials [23]. Nonetheless, much of the existing research has concentrated on expensive and engineered carbon nanostructures, which may not be feasible for large-scale applications. In this study, commercially available graphite is introduced into the epoxy matrix to fabricate graphite-reinforced epoxy composites using a solution-based approach. Subsequently, the properties of these resulting composites are meticulously examined and correlated to their morphologies. The obtained results affirm the beneficial influence of graphite not only on the thermal conductivity but also on the mechanical properties of the polymers. These findings hint at novel opportunities for crafting low-cost yet high-performing epoxy composites.

2. Materials and Methods

2.1. Sample Preparation

All the chemicals utilized in this study were procured from Sigma-Aldrich. To create graphite/epoxy composites, a scalable solution-based approach was adopted, enabling the cost-effective production of composite samples. The graphitic flakes were obtained by the mechanical exfoliation of synthetic graphite rod (Goodfellow7440-44-0, C > 99.997%) with grain sizes in the range 21–100 μm and a density of 2.27 g/cm³ using a mortar and pestle for 2 h. The powder obtained was then combined with poly (propylene glycol) bis(2-aminopropyl) ether (Jeffamine D-230) and subjected to 30 min of sonication in an ultrasonic bath. Following this, a pre-melted epoxy monomer, diglycidylether bisphenol (EPON 826), and neopentyl glycol diglycidylether (NGDE) were introduced into the mixture. The amounts of graphite flakes in the components used in the preparation of the composites are shown in Table 1. The graphite flakes were added at rates of 1%, 5%, and 10% by weight. The resulting blend was vigorously shaken to ensure a homogeneous suspension, as illustrated in Figure 1a. Subsequently, the suspension was poured into rubber molds of various shapes and cured at 100 °C for 1 h. Post-curing was then conducted at 130 °C for 1 h to produce the composite specimens for the subsequent tensile (ASTM D 412), compressive (cylindrical; diameter = 1 cm, height = 1 cm), and thermal conductivity (cylindrical; diameter = 2 cm, height = 1 cm) tests. These specimens are depicted in Figure 1b, Figure 1c, and Figure 1d, respectively. The latter set of specimens was also employed for SEM, FTIR, and XRD analyses.

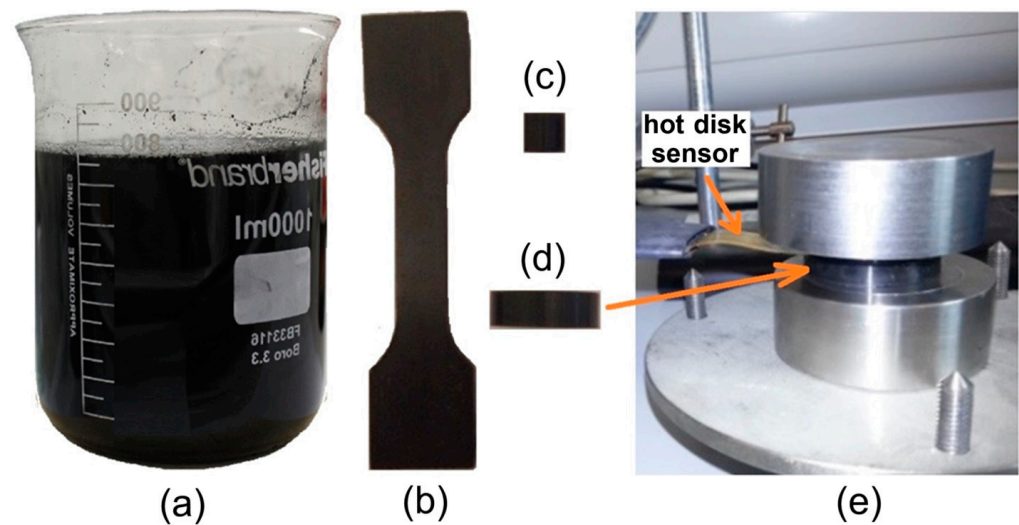


Figure 1. (a) The uniform suspension of graphite flakes, Jeffamine D-230, EPON 826, and NGDE used to prepare the samples for the (b) tensile, (c) compressive, and (d) thermal conductivity tests. (e) A close up of the setup used to measure the latter, in which a hot disk sensor is utilized.

Table 1. Quantity of the materials used for the preparation of the epoxy and composite samples, comprising epox-1 wt.% graphite (G1), epox-5 wt.% graphite (G5), and epox-10 wt.% graphite (G10).

	Epoxy	G1	G5	G10
Graphite Flake	0.00 g	0.25 g	1.23 g	2.47 g
Jeffamine D-230	6.90 g	6.90 g	6.90 g	6.90 g
EPON 826	13.17 g	13.17 g	13.17 g	13.17 g
NGDE	4.55 g	4.55 g	4.55 g	4.55 g

2.2. Characterization

Morphological examinations were conducted using a scanning electron microscope (FEI NanoSEM, USA). The cross-sections of both the pure epoxy and the graphite/epoxy samples were prepared by cutting the samples for a microscopy analysis. The compressive properties of the samples were assessed using Hounsfield equipment (Model H10KS, UK), with a cross-head rate set at 0.5 mm/min to record the strains. Compressive specimens were compressed between two steel plates, with the load applied until the specimen was compressed to approximately 25% of its original length. The tensile tests were carried out using an Instron machine (Model 5982, USA) at room temperature. Three identical specimens were employed for both tensile and compressive testing, and the mean values obtained were recorded as the final results. The thermal conductivity measurements were performed on cylindrical specimens at room temperature using a thermal conductivity meter (Hot Disk M1, Sweden). In this setup, the samples were manipulated without any further preparations beyond ensuring one plane surface on each of the two sample specimens to sandwich a Kapton-insulated sensor between them (refer to Figure 1e). At least three measurements were conducted for each specific material. The surface properties of the composites were evaluated using Fourier transform infrared spectroscopy (FTIR, Bruker Tensor 27 FTIR, Germany) within the frequency range of 500–4000 cm^{-1} utilizing cylindrical specimens. X-ray diffraction (XRD) patterns were taken on cylindrical samples using a Philips X'Pert PW3020 X-ray diffractometer (UK) with Cu $K\alpha$ radiation.

3. Results

3.1. Morphological and Structural Characterization

The morphological, mechanical, and physical changes associated with the addition of up to 10 wt% graphite flakes to epoxy were investigated in this study. The graphitic flakes were obtained by the mechanical exfoliation of a synthetic graphite rod ($C > 99.9\%$) using a mortar and pestle. In order to obtain a homogeneous distribution of graphite in epoxy, a solution-based method was successfully adapted as described in the experimental section. Figure 2 shows the SEM morphologies of the graphite powder, epoxy, and their composites produced. According to Figure 2a, the initial graphite particles were irregular in shape and highly agglomerated with a fluffy structure and large voids. The morphology of the neat epoxy, presented in Figure 2b, can be characterized by the presence of uneven surfaces with agglomerated clusters and numerous holes and gaps. Figures 2c and 2d represent the morphology of the epoxy composites containing 5 wt.% and 10 wt.% graphite additives, respectively. The morphology of these samples displays similar characteristics as observed in the neat epoxy in terms of the presence of a rough surface. However, it can be observed that the number of holes and gaps has sharply decreased by adding graphite. These textures, therefore, seem to be modified towards a more compact morphology. It was reported that the morphology of epoxy does not considerably change by the addition of 0–30 wt.% graphite filler [24]. The great performance of graphite in the morphological modification observed in this study can be attributed to the homogeneous distribution of graphite in the epoxy. The delamination nature of the graphite layers can promote the penetration of epoxy, resulting in a well-dispersed composite [25,26].

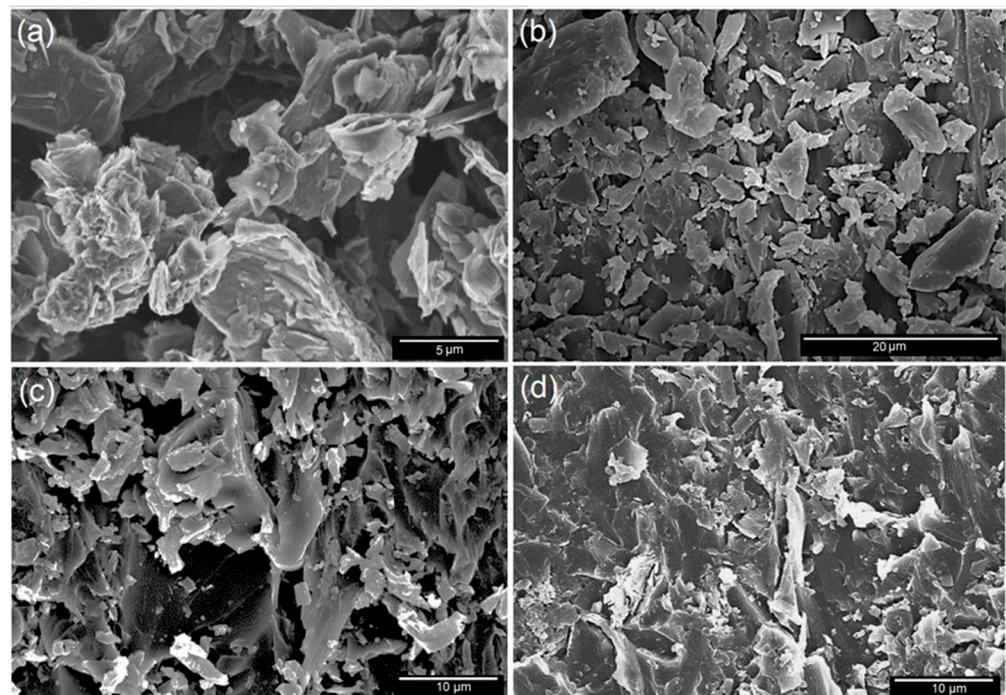


Figure 2. SEM micrographs of (a) the graphite powder used as the filler. The cross-section of (b) the epoxy and the composites produced by the addition of (c) 5 wt% and (d) 10 wt% graphite into the epoxy.

The crystalline structures of the neat epoxy, and the graphite powder and the composite containing 5wt% graphite were characterized by X-ray diffraction and the results are exhibited in Figure 3. The XRD pattern of the epoxy (Figure 3a) shows a broad peak extending from 16° to 22° which reflects the amorphous nature of the material. In contrast, the raw graphite material (Figure 3b) exhibits a sharp diffraction peak at $2\theta = 26.45^\circ$, corresponding to the (002) planes of the graphite. The diffraction pattern of the graphite/epoxy

composite (Figure 3c) is characterized by the presence of the (002) graphite reflection at the same 2θ position of 26.60° together with the broad epoxy peak, confirming the presence of the graphite with its identical hexagonal structure and the relatively same interlayer space in the composite material produced. In the XRD patterns of the graphite and the graphite/epoxy composite, the peaks observed at the two-theta values of 42.36° , 44.46° , and 54.12° can be related to the diffraction peaks originated from the (100), (101), and (004) planes of the graphite lattice, respectively. The surface characteristics of the neat epoxy and the graphite/epoxy composite containing 10 wt.% graphite was further analyzed by Fourier transform infrared spectroscopy (FTIR) at room temperature, and the spectra are shown in Figure 4. The FTIR spectrum of the neat epoxy shows the characteristic absorption peaks at 3390 cm^{-1} corresponding to the stretching vibrations of O-H, and the peaks at 2964 cm^{-1} , 2920 cm^{-1} , and 2866 cm^{-1} representing the stretching vibrations of aliphatic C-H [25]. In the case of the graphite/epoxy composite, the less intense and more broad peaks observed can be attributed to the presence of a smaller number of hydroxyl and aliphatic C-H bonds in the composite material in comparison to those of the neat epoxy, which can in turn be corresponded to the good mixing of the graphite into the polymer achieved.

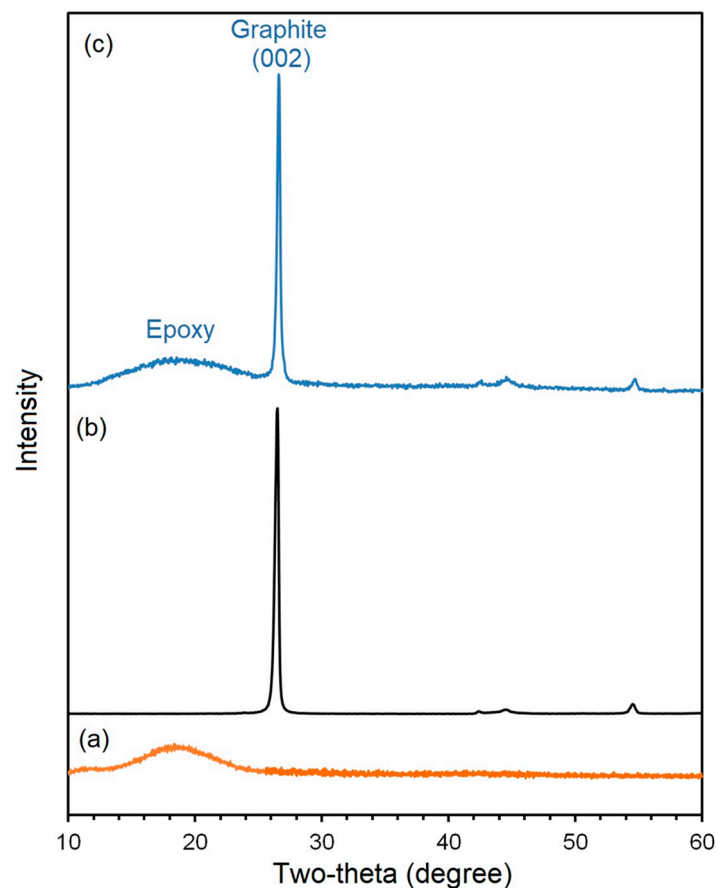


Figure 3. XRD patterns of (a) the neat epoxy, (b) the graphite powder, and (c) the graphite/epoxy composite containing 5wt% graphite.

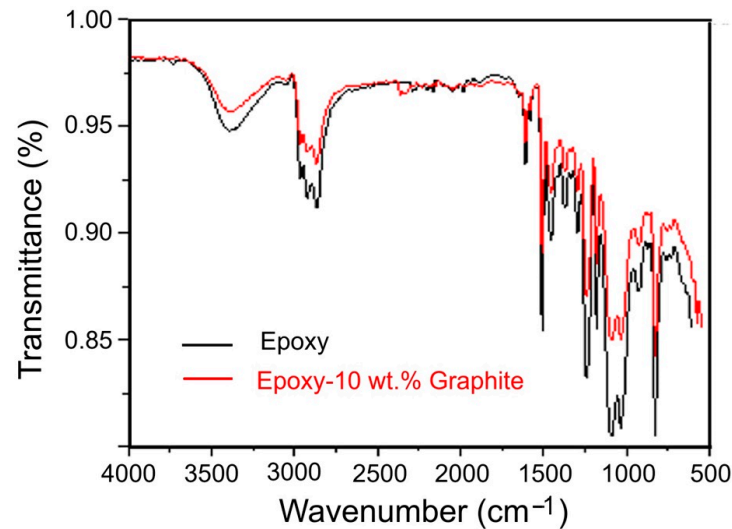


Figure 4. FTIR spectrum of unmodified epoxy resin and epoxy resin containing 10 wt% graphite flakes.

3.2. Thermal Conductivity Characterization

The morphological modification observed had an enhancing influence on the thermal conductivity of the epoxy-based materials produced, as can be seen in Table 2. It should be mentioned that epoxy resins usually display a poor thermal conductivity, and therefore, graphite derivatives, i.e., expanded graphite [26], graphene nanoplatelets [27], and graphene oxide [28], can be used to improve the thermal conductivity of epoxy. It has been reported that the thermal conductivity of carbon/epoxy composites strongly depends on the content, shape, and dispersion of the carbon filler used [29–31]. The thermal conductivity of neat epoxy could be increased by a factor of 3–7 by adding 4–20% carbon additives comprising expanded graphite [32], carbon nanotubes [19], graphite oxide [33], or exfoliated graphite [34]. In this article, we report on the thermal conductivity of graphite/epoxy composites.

Table 2. Details of the characterization results obtained using various samples.

Sample	I. Test	II. Test	III. Test	Average	Standard Deviation
Compressive strength (MPa)					
Epoxy	73	60	66	66	5
G1	72	75	70	73	2
G5	68	77	71	72	4
G10	74	75	69	73	2
Tensile strength (MPa)					
Epoxy	51	25	40	39	13
G1	41	36	36	38	3
G5	20	20	24	22	2
G10	20	19	26	22	4
Young's modulus (MPa)					
Epoxy	2951	1567	1996	2171	709
G1	3022.63	2933	2678	2878	179
G5	2143.8	2140	3159	2481	587
G10	3796.83	3779	3596	3724	111

Table 2. Cont.

Sample	I. Test	II. Test	III. Test	Average	Standard Deviation
Thermal conductivity (W/m·K)					
Epoxy	0.2220	0.2245	0.2223	0.2229	0.0011
G1	0.2786	0.2786	0.2778	0.2783	0.0004
G5	0.4951	0.4951	0.4657	0.4853	0.0139
G10	0.5807	0.5807	0.5339	0.5651	0.0221

The average values of thermal conductivity for the neat epoxy and the graphite/epoxy composites prepared in this study were measured at 0.2229, 0.2783, 0.4853, and 0.5651 W/m·K for the graphite contents of 0, 1, 5, and 10 wt.%, respectively (Figure 5a). Each measurement was conducted three times to ensure reliability, and the average values are reported. The details of the characterization results, along with the standard deviations, are presented in Table 2. The result obtained is in line with the literature [35–37] suggesting that the thermal conductivity of the composites increase with the increase in the graphite content. It should be mentioned that unlike other forms of carbon nanostructures used as the filler such as expanded graphite [38], exfoliated graphite [39], and carbon nanotubes [40], graphite is an inexpensive, sustainable, and highly available raw material [41]. Therefore, the direct application of graphite powder to fabricate epoxy composites with improved thermal conductivity is interesting for applications such as aerospace engineering [42], automotive [43], and cryogenic engineering [44].

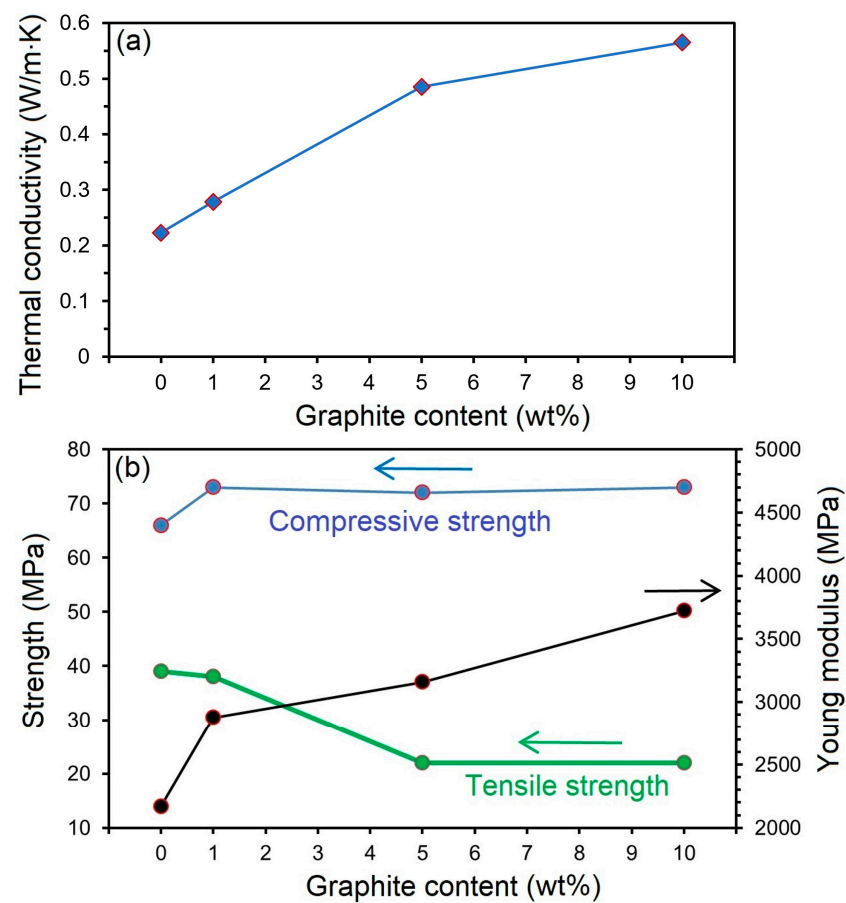


Figure 5. The properties of the graphite/epoxy composites at various graphite loading, comprising (a) the average values of thermal conductivity and (b) the average values of mechanical properties.

3.3. Characterization of Mechanical Properties

The mechanical properties of epoxy-based materials are important in structural applications. It was reported that graphite can increase the material rigidity of composites since it reduces the movement of the epoxy matrix under external forces [23]. Other carbon materials including carbon nanoparticles [45] and graphite nanoplates [46] have also been found to be able to increase the mechanical properties of epoxy. The compressive strength of the epoxy and its composites containing 1, 5, and 10 wt.% graphite was measured to have the average values of 66, 73, 72, and 73 MPa, respectively, as can be seen in Table 2 and Figure 5b. Notably, it can be observed that the compressive strength has been increased by 11% by adding only 1 wt.% graphite, providing the evidence for the appropriate mutual interaction between graphite and epoxy. This feature can be attributed to the homogeneous mixing of the components leading to the morphological modification, as observed in Figure 2. However, from Figure 5b, the further addition of graphite over 1 wt% did not show a considerable effect on the compressive strength of the resultant composites.

The values of the tensile strength of the graphite/epoxy composites, exhibited in Figure 5b, were measured to be 39, 38, 22, and 22 MPa for the composites containing 0, 1, 5, and 10 wt.% graphite additives, respectively. For the case of Young's modulus, these values were 2171, 2878, 3159, and 3724 MPa, respectively. It can be seen that by increasing the graphite loading, the value of the tensile strength decreases while that of Young's modulus increases. Accordingly, a prominent decrease in the tensile strength is observed in the composites containing 5 and 10 wt.% graphite additives. This observation can be explained based on the weak interlayer van der Waals forces in the graphite flakes used as the additive, decreasing the adhesive strength of the epoxy material, hence lowering the tensile strength.

The addition of graphite generally increases the thermal conductivity of the epoxy material. As the weight percentage of graphite increases, the thermal conductivity also increases, as seen in the values for 1 wt.% graphite (0.45 W/m·K), 5 wt.% graphite (0.97 W/m·K), and 10 wt.% graphite (1.13 W/m·K). The addition of graphite generally decreases the tensile strength of the epoxy material. This is shown by the decrease in the tensile strength from 39.00 MPa for the pure epoxy to 22.00 MPa for the epoxy with 5 wt.% graphite and 10 wt.% graphite. The addition of graphite generally increases both the compressive strength and Young's modulus of the epoxy material. As the weight percentage of graphite increases, the compressive strength and Young's modulus also increase.

The preparation of epoxy/carbon composites reported in the literature often involves expensive and complex production methods. For example, Kuo et al. [47] utilized graphitic nanoflakes (GNFs) with the thickness of 20–100 nm to create composites with compressive strengths of 73 MPa and 51 MPa at 1 wt% and 5 wt% GNF, respectively. Additionally, the thermal conductivity of epoxy composites containing 2 wt% and 4 wt% carbon has been reported to be 0.260 W/m·K and 0.319 W/m·K, respectively [48,49]. In contrast, as shown in Table 2, epoxy composites with enhanced physical and thermal properties can be produced using low-cost and widely available graphite powder as the filler material. The results indicate that by adding 5 wt% of commercially available graphite to epoxy, not only the thermal conductivity of the material increases from 0.223 to 0.485 W/m·K, but also, the compressive strength of the material improves from 66 to 72 MPa, highlighting optimal conditions where both thermal conductivity and compressive strength are critical for epoxy applications. One such application can be the thermal interface materials used in electronics, in which the epoxy composites used [50,51] require high compressive strength to maintain contact between heat-generating components and heat sinks. This ensures efficient heat transfer and stability under compressive loads, while good thermal conductivity enhances heat dissipation.

As can be realized, the tensile strength of epoxy decreases with increasing the graphitic additive content, while compressive strength tends to increase. This behavior can be attributed to the structural characteristics of the graphitic lattice, which is composed of stacked graphene layers. These layers exhibit high strength under compression due to their

ability to bear loads effectively when pressed together. However, the same graphene layers have relatively weak interlayer bonding, making them less effective under tensile stress. As more graphitic additive is introduced, the material's overall structure becomes dominated by the properties of these graphene layers of the graphite flakes, leading to improved compressive performance while compromising tensile strength. The mechanical blocking of polymer chains can also play a role in this context. It should be mentioned that bulk graphite materials may be exfoliated into highly conductive graphene nanosheets [52,53] with few stack layers, in which the influence of van der Waals forces is minimal. The effect of such graphene materials that can be fabricated using highly available low-cost resources [54,55] on the mechanical and physical properties of the resultant epoxy composite is worthy to be investigated in future studies. In particular, graphitic materials with enhanced thermal oxidation stability above 400 °C [56,57] can enhance the safety characteristics of epoxy materials.

4. Conclusions

In the present study, commercial graphite was used to prepare 1–10 wt.% graphite/epoxy composites using a simple and facile solution-based method. The microscopy studies supported by the X-ray diffraction and FTIR spectroscopic characterization of the composite materials revealed the homogeneous distribution of graphite in the epoxy to form compact composites without any obvious graphite agglomerates and voids. The XRD studies of the composites further revealed that the d-spacing of the graphite material remains unchanged upon incorporation into the epoxy. The addition of graphite caused an increase in the thermal conductivity, compressive strength, and Young's modulus of the composites. The tensile strength, however, decreased by adding graphite. The addition of 1, 5, and 10 wt% graphite to epoxy enhances the mechanical and thermal properties of the composite materials G1, G5, and G10, respectively. The compressive strength remains relatively stable across the samples, showing a slight increase with the addition of the graphite, rising from 66 MPa to 72 or 73 MPa for the composites. In contrast, the tensile strength decreases with increasing graphite content, with the pure epoxy exhibiting a mean tensile strength of 39 MPa compared to 38 MPa for G1 and 22 MPa for both G5 and G10. Young's modulus shows a significant improvement, particularly in G10, which has a mean value of 3724 MPa, indicating enhanced stiffness with higher graphite content. The thermal conductivity also increases significantly with graphite addition, reaching a maximum of 0.5651 W/m·K for G10, highlighting the potential of graphite/epoxy composites for applications requiring improved heat dissipation. Overall, the incorporation of graphite enhances the thermal and structural characteristics of epoxy, especially in terms of stiffness and conductivity. The results obtained can be used towards the preparation of low-cost epoxy-based composites with improved properties.

Author Contributions: Conceptualization, A.R.K.; methodology, A.G. and A.R.K.; software, A.G. and A.R.K.; validation, A.G. and A.R.K.; formal analysis, A.G. and A.R.K.; investigation, A.G. and A.R.K.; resources, A.R.K.; data curation, A.G. and A.R.K.; writing—original draft preparation, A.G. and A.R.K.; writing—review and editing, A.G. and A.R.K.; visualization, A.G. and A.R.K. All authors have read and agreed to the published version of the manuscript.

Funding: This work was funded by the Department of Materials Science and Metallurgy, University of Cambridge, TUBITAK (2219-International Postdoctoral Research Fellowship Program for Turkish Citizens), and the National Natural Science Foundation of China (52250610222).

Data Availability Statement: Data used has been provided in the article.

Acknowledgments: Thanks to J. Yang for assistance with conductivity measurements.

Conflicts of Interest: The authors declare no conflict of interest.

References

1. Albert, A.A.; Parthasarathy, V.; Kumar, P.S. Review on Recent Progress in Epoxy-Based Composite Materials for Electromagnetic Interference(EMI) Shielding Applications. *Polym. Compos.* **2024**, *45*, 1956–1984. [[CrossRef](#)]
2. Panta, J.; Zhang, Y.X.; Rider, A.N.; Wang, J. Ozone Functionalized Graphene Nanoplatelets and Triblock Copolymer Hybrids as Nanoscale Modifiers to Enhance the Mechanical Performance of Epoxy Adhesives. *Int. J. Adhes. Adhes.* **2022**, *116*, 103135. [[CrossRef](#)]
3. Khalid, M.Y.; Kamal, A.; Otabil, A.; Mamoun, O.; Liao, K. Graphene/Epoxy Nanocomposites for Improved Fracture Toughness: A Focused Review on Toughening Mechanism. *Chem. Eng. J. Adv.* **2023**, *16*, 100537. [[CrossRef](#)]
4. Zhang, L.; Liu, H.; Wang, Z.; Sui, W.; Gong, Y.; Cui, J.; Ao, Y.; Shang, L. Functional Boron Nitride/Graphene Oxide Three-Dimensional Skeleton Co-Heat Transfer Epoxy Resin Composite. *J. Alloys Compd.* **2024**, *985*, 173935. [[CrossRef](#)]
5. Sun, Z.; Li, J.; Yu, M.; Kathaperumal, M.; Wong, C.P. A Review of the Thermal Conductivity of Silver-Epoxy Nanocomposites as Encapsulation Material for Packaging Applications. *Chem. Eng. J.* **2022**, *446*, 137319. [[CrossRef](#)]
6. Chen, Y.; Shi, C.; Guo, X.; Qing, C.; Zou, D. A Metal-Based Microencapsulated Phase Change Material (MEPCM) with High Thermal Conductivity, Electrical Insulation and Flame Retardancy and Its Application in Epoxy Resin. *Compos. Part A Appl. Sci. Manuf.* **2024**, *180*, 108081. [[CrossRef](#)]
7. Kim, C.S.; Jang, J.; Im, H.G.; Yoon, S.; Kang, D.J. Preparation and Performance of Alumina/Epoxy-Siloxane Composites: A Comparative Study on Thermal- and Photo-Curing Process. *Heliyon* **2024**, *10*, e27580. [[CrossRef](#)]
8. Zhou, Z.; Huang, R.; Liu, H.; Zhao, Y.; Miao, Z.; Wu, Z.; Zhao, W.; Huang, C.; Li, L. Dielectric AlN/Epoxy and SiC/Epoxy Composites with Enhanced Thermal and Dynamic Mechanical Properties at Low Temperatures. *Prog. Nat. Sci. Mater. Int.* **2022**, *32*, 304–313. [[CrossRef](#)]
9. Adeli, R.; Shirmardi, S.P.; Ahmadi, S.J. Neutron Irradiation Tests on B4C/Epoxy Composite for Neutron Shielding Application and the Parameters Assay. *Radiat. Phys. Chem.* **2016**, *127*, 140–146. [[CrossRef](#)]
10. Watpade, A.D.; Thakor, S.; Jain, P.; Mohapatra, P.P.; Vaja, C.R.; Joshi, A.; Shah, D.V.; Tariqul Islam, M. Comparative Analysis of Machine Learning Models for Predicting Dielectric Properties in MoS2 Nanofiller-Reinforced Epoxy Composites. *Ain Shams Eng. J.* **2024**, *15*, 102754. [[CrossRef](#)]
11. Li, G.; Chen, L.; An, Y.; Gao, M.; Zhou, H.; Chen, J. Investigating the Effect of Polytetrafluoroethylene on the Tribological Properties and Corrosion Resistance of Epoxy/Hydroxylated Hexagonal Boron Nitride Composite Coatings. *Corros. Sci.* **2023**, *210*, 110820. [[CrossRef](#)]
12. Kim, J.W.; Gardner, J.M.; Sauti, G.; Jensen, B.D.; Wise, K.E.; Wincheski, R.A.; Smith, J.G.; Zavada, S.R.; Siochi, E.J. Fabrication of Carbon Nanotube Epoxy Prepreg towards Lightweight Structural Composites. *Compos. Part B Eng.* **2024**, *275*, 111329. [[CrossRef](#)]
13. Hao, Q.; Liu, S.; Wang, X.; Zhang, P.; Mao, Z.; Zhang, X. Progression from Graphene and Graphene Oxide to High-Performance Epoxy Resin-Based Composite. *Polym. Degrad. Stab.* **2024**, *223*, 110731. [[CrossRef](#)]
14. Bao, D.; Gao, Y.; Cui, Y.; Xu, F.; Shen, X.; Geng, H.; Zhang, X.; Lin, D.; Zhu, Y.; Wang, H. A Novel Modified Expanded Graphite/Epoxy 3D Composite with Ultrahigh Thermal Conductivity. *Chem. Eng. J.* **2022**, *433*, 133519. [[CrossRef](#)]
15. Chow, D.; Burns, N.; Boateng, E.; van der Zalm, J.; Kycia, S.; Chen, A. Mechanical Exfoliation of Expanded Graphite to Graphene-Based Materials and Modification with Palladium Nanoparticles for Hydrogen Storage. *Nanomaterials* **2023**, *13*, 2588. [[CrossRef](#)]
16. Kamali, A.R.; Fray, D. Electrochemical interaction between graphite and molten salts to produce nanotubes, nanoparticles, graphene and nanodiamonds. *J. Material. Sci.* **2016**, *51*, 569–576. [[CrossRef](#)]
17. Lee, C.-S.; Shim, S.J.; Kim, T.H. Scalable Preparation of Low-Defect Graphene by Urea-Assisted Liquid-Phase Shear Exfoliation of Graphite and Its Application in Doxorubicin Analysis. *Nanomaterials* **2020**, *10*, 267. [[CrossRef](#)]
18. Kim, S.H.; Jiang, S.; Lee, S.-S. Direct CVD Growth of Transferable 3D Graphene for Sensitive and Flexible SERS Sensor. *Nanomaterials* **2023**, *13*, 1029. [[CrossRef](#)]
19. Mousavi, S.R.; Estaji, S.; Kiaei, H.; Mansourian-Tabaei, M.; Nouranian, S.; Jafari, S.H.; Ruckdäschel, H.; Arjmand, M.; Khonakdar, H.A. A Review of Electrical and Thermal Conductivities of Epoxy Resin Systems Reinforced with Carbon Nanotubes and Graphene-Based Nanoparticles. *Polym. Test.* **2022**, *112*, 107645. [[CrossRef](#)]
20. Luo, F.; Wu, K.; Wang, S.; Lu, M. Melamine Resin/Graphite Nanoflakes Hybrids and Its Vacuum-Assisted Prepared Epoxy Composites with Anisotropic Thermal Conductivity and Improved Flame Retardancy. *Compos. Sci. Technol.* **2017**, *144*, 100–106. [[CrossRef](#)]
21. Owais, M.; Zhao, J.; Imani, A.; Wang, G.; Zhang, H.; Zhang, Z. Synergetic Effect of Hybrid Fillers of Boron Nitride, Graphene Nanoplatelets, and Short Carbon Fibers for Enhanced Thermal Conductivity and Electrical Resistivity of Epoxy Nanocomposites. *Compos. Part A Appl. Sci. Manuf.* **2019**, *117*, 11–22. [[CrossRef](#)]
22. Mishra, S.; Pratap, V.; Chaurasia, A.K.; Soni, A.K.; Dubey, A.; Dixit, A.K. Combined Effect of Exfoliated Graphite/Ferrite Filled Epoxy Composites on Microwave Absorbing and Mechanical Properties. *Phys. Open* **2023**, *14*, 100138. [[CrossRef](#)]
23. Suherman, H.; Dweiri, R.; Sulong, A.B.; Zakaria, M.Y.; Mahyoedin, Y. Improvement of the Electrical-Mechanical Performance of Epoxy/Graphite Composites Based on the Effects of Particle Size and Curing Conditions. *Polymers* **2022**, *14*, 502. [[CrossRef](#)]
24. Baptista, R.; Mendão, A.; Rodrigues, F.; Figueiredo-Pina, C.G.; Guedes, M.; Marat-Mendes, R. Effect of High Graphite Filler Contents on the Mechanical and Tribological Failure Behavior of Epoxy Matrix Composites. *Theor. Appl. Fract. Mech.* **2016**, *85*, 113–124. [[CrossRef](#)]

25. Ni, Y.; Pu, Y.; Zhang, J.; Cui, W.; Gao, M.; You, D. Charged Functional Groups Modified Porous Spherical Hollow Carbon Material as CDI Electrode for Salty Water Desalination. *J. Environ. Sci.* **2025**, *149*, 254–267. [[CrossRef](#)]
26. Feng, W.; Liang, B.; Chen, J.; Gao, X.; Yao, D.; Lu, C.; Pang, X. Tribological performance of epoxy composites reinforced by 3D expanded graphite skeleton containing oil microcapsules. *Tribol. Int.* **2024**, *197*, 109814. [[CrossRef](#)]
27. Srivastava, A.K.; Yerramalli, C.S.; Singh, A. Static and fatigue performance of graphene nanoplatelets coated bi-directional carbon fiber-epoxy composites under bending loads. *J. Appl. Polym.* **2024**, *141*, e55830. [[CrossRef](#)]
28. Wang, P.; Zhang, S.; Hu, X.; Leng, Y.; Li, X.; Tao, B.; Xu, M. Constructing piperazine pyrophosphate@LDH@rGO with hierarchical core-shell structure for improving thermal conductivity, flame retardancy and smoke suppression of epoxy resin thermosets. *Compos. B* **2024**, *287*, 111870. [[CrossRef](#)]
29. Huang, X.; Zhi, C.; Lin, Y.; Bao, H.; Wu, G.; Jiang, P.; Mai, Y.W. Thermal Conductivity of Graphene-Based Polymer Nanocomposites. *Mater. Sci. Eng. R Reports* **2020**, *142*, 100577. [[CrossRef](#)]
30. Guo, X.; Cheng, S.; Cai, W.; Zhang, Y.; Zhang, X.-A. A Review of Carbon-Based Thermal Interface Materials: Mechanism, Thermal Measurements and Thermal Properties. *Mater. Des.* **2021**, *209*, 109936. [[CrossRef](#)]
31. Liu, Y.; Chen, B.; Wu, K.; Lu, M.; Jiao, E.; Shi, J.; Lu, M. Ultrahigh Thermal Conductivity of Epoxy Composites Based on Curling Bioinspired Functionalized Graphite Films for Thermal Management Application. *Compos. Part A Appl. Sci. Manuf.* **2021**, *146*, 106413. [[CrossRef](#)]
32. Wang, Z.; Qi, R.; Wang, J.; Qi, S. Thermal Conductivity Improvement of Epoxy Composite Filled with Expanded Graphite. *Ceram. Int.* **2015**, *41*, 13541–13546. [[CrossRef](#)]
33. Aradhana, R.; Mohanty, S.; Nayak, S.K. Novel Electrically Conductive Epoxy/Reduced Graphite Oxide/Silica Hollow Microspheres Adhesives with Enhanced Lap Shear Strength and Thermal Conductivity. *Compos. Sci. Technol.* **2019**, *169*, 86–94. [[CrossRef](#)]
34. Guo, X.; Zheng, K.; Shi, H.; Chen, L.; Shen, Y.; Chen, J.; Tao, X.; Yu, M. Thermal Regulation of Photovoltaic Panels Using Shape-Stabilized Phase Change Materials Supported by Exfoliated Graphite/Graphene Nanofillers. *J. Clean. Prod.* **2024**, *446*, 141435. [[CrossRef](#)]
35. Sanghvi, M.R.; Tambare, O.H.; More, A.P. *Performance of Various Fillers in Adhesives Applications: A Review*; Springer: Berlin/Heidelberg, Germany, 2022; Volume 79, ISBN 0028902104022.
36. Depaifve, S.; Hermans, S.; Ruch, D.; Laachachi, A. Combination of Micro-Computed X-Ray Tomography and Electronic Microscopy to Understand the Influence of Graphene Nanoplatelets on the Thermal Conductivity of Epoxy Composites. *Thermochim. Acta* **2020**, *691*, 178712. [[CrossRef](#)]
37. Lian, G.; Tuan, C.C.; Li, L.; Jiao, S.; Wang, Q.; Moon, K.S.; Cui, D.; Wong, C.P. Vertically Aligned and Interconnected Graphene Networks for High Thermal Conductivity of Epoxy Composites with Ultralow Loading. *Chem. Mater.* **2016**, *28*, 6096–6104. [[CrossRef](#)]
38. Kamali, A.R. Eco-Friendly Production of High Quality Low Cost Graphene and Its Application in Lithium Ion Batteries. *Green Chem.* **2016**, *18*, 1952–1964. [[CrossRef](#)]
39. La, L.B.T.; Nguyen, H.; Tran, L.C.; Su, X.; Meng, Q.; Kuan, H.-C.; Ma, J. Exfoliation and Dispersion of Graphene Nanoplatelets for Epoxy Nanocomposites. *Adv. Nanocomposites* **2024**, *1*, 39–51. [[CrossRef](#)]
40. Mohammad, H.; Stepashkin, A.A.; Tcherdyntsev, V.V. Effect of Graphite Filler Type on the Thermal Conductivity and Mechanical Behavior of Polysulfone-Based Composites. *Polymers* **2022**, *14*, 399. [[CrossRef](#)]
41. Wu, S.; Li, T.; Tong, Z.; Chao, J.; Zhai, T.; Xu, J.; Yan, T.; Wu, M.; Xu, Z.; Bao, H.; et al. High-Performance Thermally Conductive Phase Change Composites by Large-Size Oriented Graphite Sheets for Scalable Thermal Energy Harvesting. *Adv. Mater.* **2019**, *31*, 1905099. [[CrossRef](#)]
42. Wu, X.; Tang, B.; Chen, J.; Shan, L.; Gao, Y.; Yang, K.; Wang, Y.; Sun, K.; Fan, R.; Yu, J. Epoxy Composites with High Cross-Plane Thermal Conductivity by Constructing All-Carbon Multidimensional Carbon Fiber/Graphite Networks. *Compos. Sci. Technol.* **2021**, *203*, 108610. [[CrossRef](#)]
43. Kim, S.H.; Park, S.J.; Lee, S.Y.; Park, S.J. Amine Functionalization on Thermal and Mechanical Behaviors of Graphite Nanofibers-Loaded Epoxy Composites. *J. Mater. Sci. Technol.* **2023**, *151*, 80–88. [[CrossRef](#)]
44. Krzak, A.; Nowak, A.J.; Frolec, J.; Králík, T.; Kotyk, M.; Boroński, D.; Matula, G. Analysis of Mechanical Properties and Thermal Conductivity of Thin-Ply Laminates in Ambient and Cryogenic Conditions. *Materials* **2024**, *17*, 5419. [[CrossRef](#)]
45. Zotti, A.; Zuppolini, S.; Borriello, A.; Zarrelli, M. Polymer Nanocomposites Based on Graphite Nanoplatelets and Amphiphilic Graphene Platelets. *Compos. Part B Eng.* **2022**, *246*, 110223. [[CrossRef](#)]
46. Mohammadi, S.; Babaei, A. Poly (Vinyl Alcohol)/Chitosan/Polyethylene Glycol-Assembled Graphene Oxide Bio-Nanocomposites as a Prosperous Candidate for Biomedical Applications and Drug/Food Packaging Industry. *Int. J. Biol. Macromol.* **2022**, *201*, 528–538. [[CrossRef](#)]
47. Kuo, W.; Wu, T.; Lu, H.; Lo, T. Microstructures and Mechanical Properties of Nano-Flake Graphite Composites. In Proceedings of the 16th International Conference on Composite Material, Kyoto, Japan, 6–13 July 2007.
48. Isarn, I.; Bonnaud, L.; Massagués, L.; Serra, À.; Ferrando, F. Enhancement of Thermal Conductivity in Epoxy Coatings through the Combined Addition of Expanded Graphite and Boron Nitride Fillers. *Prog. Org. Coatings* **2019**, *133*, 299–308. [[CrossRef](#)]
49. Ganguli, S.; Roy, A.K.; Anderson, D.P. Improved Thermal Conductivity for Chemically Functionalized Exfoliated Graphite/Epoxy Composites. *Carbon N. Y.* **2008**, *46*, 806–817. [[CrossRef](#)]

50. Liu, Z.; Wang, M.; Wang, T.; Tian, Y.; Cheng, J. Epoxy Resin-Based Gel Phase Change Material for Strong Interface Bonding and Interface Thermal Management. *Chem. Mater.* **2024**, *36*, 9414–9423. [[CrossRef](#)]
51. Zheng, K.; Li, Z.; Wang, J.; Nie, S.; Guo, S.; Zhang, X. Electrothermal Curable Epoxy Interface Adhesive Composite with Low Voltage: An Ideal Thermal Management and EMI Shielding Material. *Ind. Eng. Chem.* **2024**, *63*, 14165–14175. [[CrossRef](#)]
52. Kamali, A.R. Clean Production and Utilisation of Hydrogen in Molten Salts. *RSC Adv.* **2020**, *10*, 36020–36030. [[CrossRef](#)]
53. Kamali, A.R. *Green Production of Carbon Nanomaterials in Molten Salts and Applications*; Springer: Singapore, 2020; ISBN 9789811523731.
54. He, Z.-K.; Sun, Q.; Xie, K.; Shi, Z.; Kamali, A.R. Reactive molten salt synthesis of natural graphite flakes decorated with SnO₂ nanorods as high performance, low cost anode material for lithium ion batteries. *J. Alloys Compd.* **2019**, *792*, 1213–1222. [[CrossRef](#)]
55. Jara, A.D.; Betemariam, A.; Woldetinsae, G.; Kim, J.Y. Purification, application and current market trend of natural graphite: A review. *Int. J. Mining Sci. Technol.* **2019**, *29*, 671–689. [[CrossRef](#)]
56. Kamali, A.R.; Divitini, G.; Schwandt, C.; Fray, D.J. Correlation between microstructure and thermokinetic characteristics of electrolytic carbon nanomaterials. *Corros. Sci.* **2012**, *64*, 90–97. [[CrossRef](#)]
57. Kamali, A.R.; Schwandt, C.; Fray, D.J. On the oxidation of electrolytic carbon nanomaterials. *Corros. Sci.* **2012**, *54*, 307–331. [[CrossRef](#)]

Disclaimer/Publisher's Note: The statements, opinions and data contained in all publications are solely those of the individual author(s) and contributor(s) and not of MDPI and/or the editor(s). MDPI and/or the editor(s) disclaim responsibility for any injury to people or property resulting from any ideas, methods, instructions or products referred to in the content.